PAPER

Spatial Fading Simulator Using a Cavity-Excited Circular Array (CECA) for Performance Evaluation of Antenna Arrays

Chulgyun PARK[†a)], ***Student Member***, **Jun-ichi TAKADA**[†], **Kei SAKAGUCHI**[†], ***and*** **Takashi OHIRA**[††], ***Members***

SUMMARY In this paper we propose a novel spatial fading simulator to evaluate the performance of an array antenna and show its spatial stochastic characteristics by computer simulation based on parameters verified by experimental data. We introduce a cavity-excited circular array (CECA) as a fading simulator that can simulate realistic mobile communication environments. To evaluate the antenna array, two stochastic characteristics are necessary. The first one is the fading phenomenon and the second is the angular spread (AS) of the incident wave. The computer simulation results with respect to fading and AS show that CECA works well as a spatial fading simulator for performance evaluation of an antenna array. We first present the basic structure, features and design methodology of CECA, and then show computer simulation results of the spatial stochastic characteristics. The results convince us that CECA is useful to evaluate performance of antenna arrays.

key words: *spatial fading simulator, cavity, CECA, antenna array performance evaluation*

1. Introduction

Recently, in wireless communication fields, antenna array systems occupy an important position. To evaluate these antenna array systems, we make efforts at obtaining reasonable results. However, testing of mobile radio transmission techniques in the field is time-consuming and often inconclusive, due to uncertainties in the statistical signal variations actually encountered. If we can reproduce the mobile communication environment at a laboratory or anechoic chamber so that it provides the average mobile communication environment verified theoretically and observed experimentally, it may be an attractive alternative [1]. Therefore, we need a standard mobile communication environment, which provides suitable conditions for mobile radio transmission experiments. The received signal has two main features: fading and spatial characteristics. The fading phenomena occur when received signals become weak, below some level, instantaneously due to phase superposition of waves coming through multi-path and this level variation follows Rayleigh distribution. In spatial characteristics, there are two properties, namely nominal direction of arrival (DoA) and angular spread (AS). If we can emulate fading and AS as observed in a real mobile communication environment, it seems quite all right to consider that emulated environment is close to the real mobile communication environment.

There are several approaches to generate fading signals. First is a stored channel approach in which actual fading fluctuations are stored in the memory [2]. Second is the so called "Jakes type" fading simulator in which a steady signal is split into several paths, each of which suffers from different Doppler shifts, and they are combined again to generate the fading [1]. Third is the Gaussian amplitude modulation of the in-phase and quadrature components of a steady carrier which can be used to provide uniform phase modulation and Rayleigh envelope fading [3].

Since the conventional fading simulators can only work in the delay and Doppler domains, it is not proper to evaluate antenna array systems. To overcome this problem, a fading emulator called a field simulator has been proposed. For mobile terminals, a field simulator composed of a phased array antenna and the shielded box is used [4]. For base stations, another field simulator using the moving metal bars is used to realize the finite angular spread [5]. Yet another field emulator using electronically steerable passive array radiator (ESPAR) antenna has recently been proposed by the authors [6], [7]. ESPAR field simulator works well as a spatial fading emulator with low cost and has a simple structure but only a small AS could be generated under specific conditions. We therefore propose a cavity-excited circular array (CECA) as a spatial fading simulator which can overcome small ASs and specific conditions. The proposed structure uses a radial cavity as a feeding circuit so that the fundamental size limitation of an ESPAR antenna can be overcome, and we can obtain wider AS. In the proposed structure, the feed probe is not directly connected to the antenna element but through a radial cavity so that the dominant radiator does not exist, which provides suitable condition for Rayleigh fading environment. In this paper we introduce CECA and show the spatial stochastic characteristics by computer simulation.

In Sect. 2, we introduce the concept, methodology, design and characteristics of CECA. In Sect. 3, we show the scenario for computer simulation and investigation of the terms to verify Rayleigh fading and AS. And next, computer simulation results will be shown on each terms and a conclusion will be made.

Manuscript received March 9, 2005.
Manuscript revised July 8, 2005.

[†]The authors are with the Graduate School of Science and Engineering, Tokyo Institute of Technology, Tokyo, 152-8552 Japan.
[††]The author is with ATR Adaptive Communications Research Labs., Kyoto-fu, 619-0028 Japan.
a) E-mail: cgpark@ap.ide.titech.ac.jp

DOI: 10.1093/ietcom/e89–b.3.906

2. Cavity-Excited Circular Array (CECA)

2.1 Concept

Figure 1 shows the fundamental structure of CECA. In this example, the array is composed of six reactance-loaded monopole elements arranged concentrically for structural symmetry, and one feed pin at the center of the radial cavity. In appearance, the reactance-loaded elements seem to be parasitic elements, but, in this structure, contrary to the ESPAR antenna, these elements are not the parasitic elements in the sense that they are fed via the radial cavity. The radial cavity may be regarded as a feed circuit and the elements above the radial cavity are fed through the radial cavity with pins connected to the reactance elements.

Fading and AS can be realized as follows. With respect to the fading, each of the fed elements has different phase due to the varied excitation coefficient by controlling the load impedance as well as the generation of higher order modes in the radial cavity. This quasi-random phase generates the Rayleigh fading. In other words, six array elements work as the local scatterers. While the ESPAR antenna produces Rayleigh fading only under specific conditions due to the fed element, CECA has more flexibility because no direct wave exists. With respect to the AS, this structure is advantageous in the sense that the excitation strength of the array elements is almost independent of the size of the radial cavity, as these elements are fed by the radial cavity and not by the proximity coupling. Therefore, this structure can achieve a wider AS than what an ESPAR antenna can achieve. Selection of the appropriate size of the radial cavity and array would easily control the AS.

2.2 Parameters

The key parameters are the height of the circular cavity, radius of CECA and positions of array elements. Figure 2 shows the structure and coordinate of CECA including cavity radius r_c, distance of antenna element from center r_a, array element length l and radial cavity height h.

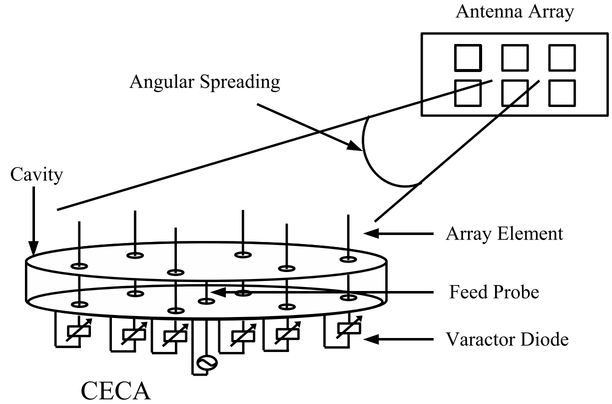

Fig. 1 Structure of CECA.

Height of Circular Cavity

As mentioned in the previous section, radial cavity plays the role of feed circuit. Therefore, the height of the circular cavity is designed to be sufficiently low so that the current distribution on array elements inside the cavity is almost uniform along the z-axis, but not so low that the return loss becomes extremely worse. This also provides convenience to design CECA because low cavity hight causes the electric field in cavity to be in uniform distribution, which means eigen mode number of z component is zero so that many of eletromagnetic field components are eliminated.

Radius of CECA

The electromagnetic fields of TM_{mnl} mode in the cavity satisfy

$$E_\rho(\rho,\phi,z) = -A\frac{k_z\lambda_{mn}}{k_\beta}J'_m(\lambda_{mn}\rho)\cos m\phi\sin k_z z, \tag{1}$$

$$E_\phi(\rho,\phi,z) = A\frac{k_z m}{k_\beta}J_m(\lambda_{mn}\rho)\sin m\phi\sin k_z z, \tag{2}$$

$$E_z(\rho,\phi,z) = A\frac{\lambda_{mn}^2}{k_\beta}J_m(\lambda_{mn}\rho)\cos m\phi\cos k_z z, \tag{3}$$

$$H_\rho(\rho,\phi,z) = -jA\frac{m}{\rho}J_m(\lambda_{mn}\rho)\sin m\phi\cos k_z z, \tag{4}$$

$$H_\phi(\rho,\phi,z) = -jA\lambda_{mn}J'_m(\lambda_{mn}\rho)\cos m\phi\cos k_z z, \tag{5}$$

$$H_z(\rho,\phi,z) = 0, \tag{6}$$

where

$$A = -\sqrt{\frac{\varepsilon}{\pi h}}\frac{1}{p_{mn}J_{m+1}(p_{mn})},$$
$$\lambda_{mn} = \frac{p_{mn}}{r_c},$$
$$k_z = \frac{l\pi}{h},$$
$$k_\beta^2 = \lambda_{mn}^2 + k_z^2,$$

and r_c, r_a, h, ε and p_{mn} represent cavity radius, distance of array element from center, height of CECA, permittivity in free space and the nth roots of $J_m = 0$ respectively. The feed

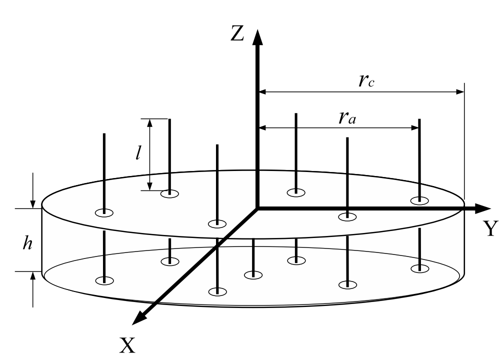

Fig. 2 Cartesian coordinate in fabrication.

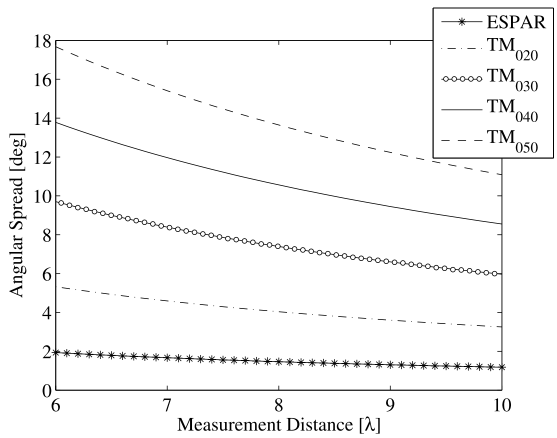

Fig. 3 AS vs. measurement distance and cavity mode.

post of CECA connected to the upper wall of the cavity at the center and small height of the cavity make CECA work in the TM_{0n0} mode so that we derive

$$E_\rho = 0 \tag{7}$$
$$E_\phi = 0 \tag{8}$$
$$E_z(\rho) = A\lambda_{0n}J_0(\lambda_{0n}\rho) \tag{9}$$
$$H_\rho = 0 \tag{10}$$
$$H_\phi(\rho) = -jA\lambda_{0n}J_0'(\lambda_{0n}\rho) \tag{11}$$
$$H_z = 0. \tag{12}$$

We obtain a suitable radius of CECA with boundary condition, $r_c = 0.4357\lambda, 1\lambda, 1.5678\lambda, \ldots$.

Position of Array Element

We locate array elements at the point of the strongest current so that the energy is able to emit at its maximum. It should also be a null point of the H field. Therefore, we have $r_a = 0.694\lambda, 1.271\lambda, \ldots$. The position of the array elements are determined by the cavity mode. Namely, the mode of the cavity decides the area of effective scatterers and its radius affects AS. Figure 3 shows that AS defined by its standard deviation varies with measurement distance and cavity mode when array length is fixed. Accordingly as measurement distance increases AS decreases, while as cavity mode increases, AS increases. We design TM_{020} mode cavity to satisfy about 5° AS because high mode cavity over TM_{020} mode is too big to handle. Figure 3 also shows the AS variation of ESPAR antenna according to measurement distance. We know that CECA has wider AS than ESPAR antenna in Fig. 3.

Length of Array Element

We designed the CECA to work in the TM_{020} mode at 2.5 GHz so that we chose the case of $r_c = 1\lambda$, $r_a = 0.694\lambda$. Table 1 defines dimensions of CECA based on theoretical value. Figure 4 shows the fabricated CECA and Fig. 5 shows a comparison of the simulation and experiment results when

Table 1 Structural dimensions of CECA.

r_c	r_a	l	h	
1.0	0.694	0.208	0.1	λ(2.5 GHz)
12.0	8.3	2.5	1.2	cm

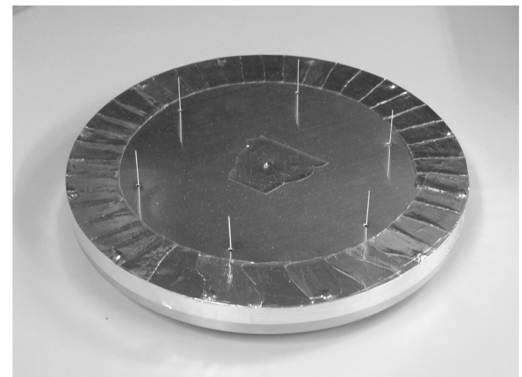

Fig. 4 Prototype CECA.

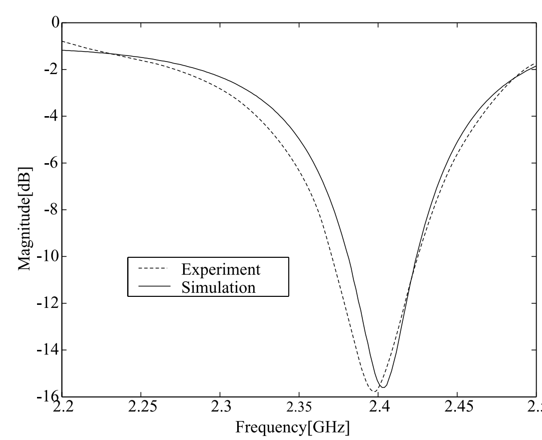

Fig. 5 Comparison of return loss between simulation and experiment.

50 Ω dummy is loaded to each array element. As the numerical analysis method, we made use of the Method of Moment (MoM) simulator FEKO [8]. Though we designed the CECA to work at 2.5 GHz, the experimental and simulation results show the little different resonance frequency due to the perturbation from antenna element. However, it becomes clear that the model used in simulation is suitable for fabrication. Though return loss is not important because CECA is not an antenna but a spatial fading simulator, note that the return loss changes according to the variation of reactance elements, and its optimization for some criterion case is not effective. We compare return loss in order to confirm the validity of the model used in simulation. From now, we utilize the values derived by this simulator. The array element will emit energy well when the element length is set to be resonant. However, the phase variation range on array elements by varying the reactance of the varactor loaded at the array elements is a more important factor since we expect CECA to work as a fading emulator and to adjust the length of the array element is the easiest way to real-

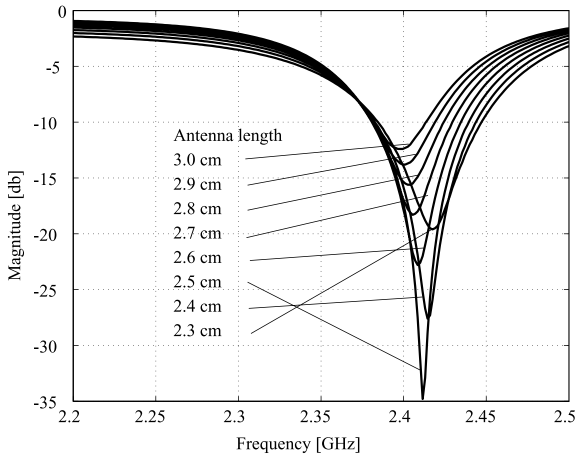

Fig. 6 Variation of return loss with element length l on simulation when 50 Ω dummy is loaded to array element. Only the length of array elements are varied and the element position parameters r_c, r_a are kept constant as 12 cm, 8.3 cm respectively.

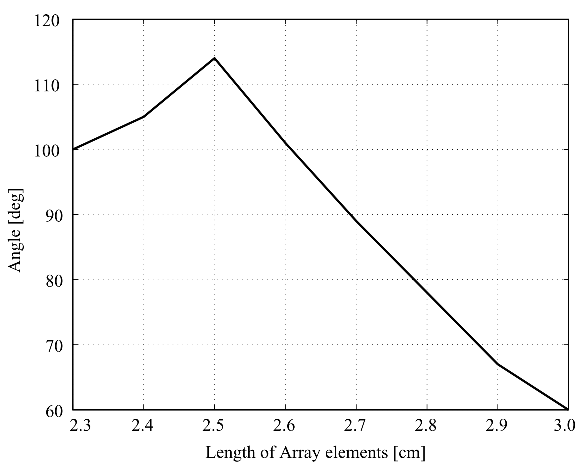

Fig. 7 Phase variation range vs. antenna length at 2.41 GHz.

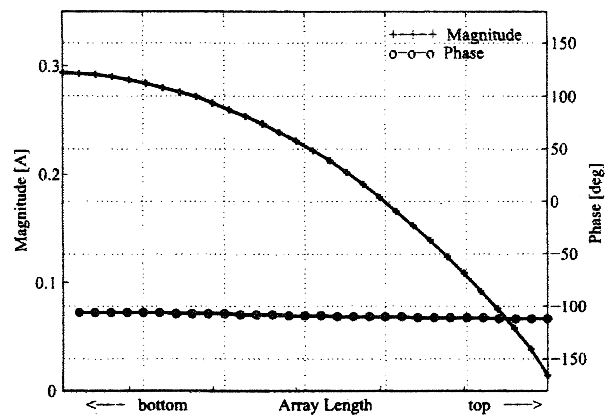

Fig. 8 Current distribution on array elements when no varactors are loaded.

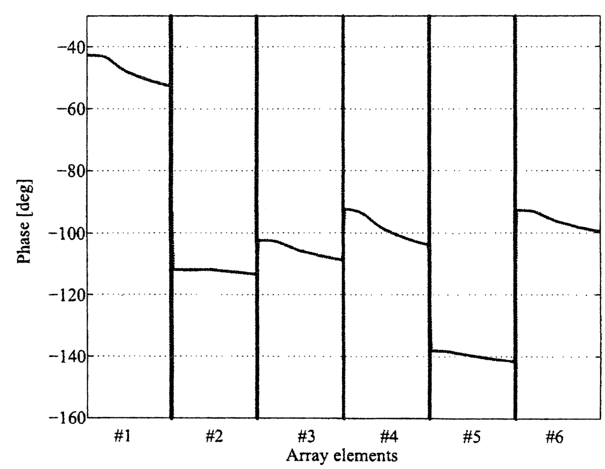

Fig. 9 Phase on each array element when random varactors are loaded.

ize it. Figure 6 depicts how we choose the element length and operating frequency. With varying element lengths, we decide the operation frequency at which the gradient of return loss becomes steep, where impedance is most sensitive to the length of the array element, which means impedance changes rapidly on the smithchart. Beside, return loss becomes better. Therefore, we know that the impedance varies widely when the array length is 25 mm as shown in Fig. 6. The impedance variation relates to the phase variation directly. Figure 7 shows the range of phase variation according to the length of array element when 50 Ω dummy is loaded instead of the reactance element. We notice that the phase variation is at the maximum when the length of array element is 25 mm as mentioned above.

2.3 Reactance Domain

In this part, we show the characteristics of CECA in the reactance domain with simulation results [9]. It is necessary to verify the variation of phase on the array elements in case of loading varactors at all array elements. We assume that the capacitance of the varactor could be varied in the range of 0.5–9 pF based on model 1SV287 made by TOSHIBA, which correspond to −132.63 Ω - −7.37 Ω at 2.41 GHz theoretically. The phases of array elements vary in more complicated manner than just the phase rotation due to reactance because of mutual coupling between array elements both inside and outside of the cavity, as well as the generation of higher modes in the cavity. Figure 8 shows the current distribution on array elements when all the reactance elements are replaced by 50 Ω dummys. In the case, all the elements have the same current distribution due to a symmetric structure. The current shown in Fig. 8 is definitely correct because of its sinusoidal amplitude which satisfies boundary condition and constant phase for array elements. Next, we change the reactance of the varactor at random. Figure 9 shows an example of the phase variation of the array element when 0.5 pF, 9 pF, 4.7 pF, 1 pF, 2.8 pF and 7.3 pF are respectively loaded and the phase values on the array elements varying. If the CECA does not resonate, the traveling wave occurs from cavity so that though the capacitance is fixed, the phase varies with the length of array element. The different capacitance causes the different variation range of phase because the different capacitances loaded at each array element cause a different electric length. The vertical axis shows the variation of the phase of current. The horizontal axis is divided into 6 segments corresponding to array element #1 to #6. Each segment denotes the length of each array element. The leftmost portion of each segment corresponds to the varactor loaded point of the array element, while the rightmost portion corresponds to the top position of the array element. We will show later that this random phase variation shall cause the Rayleigh fading.

3. Fading Simulation

3.1 Modeling

We obtain impedance $[Z_c]$ by simulation when the varactors have not been loaded.

$$[Z_c][I] = [V] \tag{13}$$

where $[Z_c][I]$ and $[V]$ denote the impedance matrix, current vector and voltage vector respectively. They are all defined at the coaxial terminals at the bottom of the cavity. When varactors have been loaded, impedance Z_{va} is added to impedance $[Z_c]$ to obtain the current distribution. When the varactors are connected,

$$[Z_c + Z_{va}][I] = [V_0]. \tag{14}$$

Z_{va} is a diagonal matrix having elements

$$[Z_{va}]_{mm} = \frac{1}{j2\pi f_c C(t)}, \tag{15}$$

$$\frac{1}{C(t)} = \frac{1}{2}\left(\frac{1}{C_{\min}} - \frac{1}{C_{\max}}\right)(\cos(2\pi f_m t + \phi_m) + 1) + \frac{1}{C_{\max}} \tag{16}$$

and V_0, f_c and f_m denote the external applied voltage, the carrier frequency and the Doppler frequency. Minimum and maximum values of capacitance are $C_{\min}$ and $C_{\max}$. Note that $C_{\min} = 0.5$ pF and $C_{\max} = 9$ pF, as described in Sect. 2.3. The subscript mm of $[Z_{va}]_{mm}$ denotes square matrix with m by m diagonal element determined by the number of array elements. The reactance values of each array element vary as in (16) when the capacitance of the varactors is varied in the range of $C_{\min}$ to $C_{\max}$. The reactance variation causes the phase variation. We vary the bias voltage to satisfy (16). In (16), the varactor values of each array element vary with different Doppler frequency, similar to Jakes model [1]. The Doppler frequency is according to the following.

$$f_m = f_D \cos(\theta_m), \tag{17}$$

where f_D is the maximum Doppler frequency and θ_m is the virtual angle between the m-th direction of departure from the mobile terminal and the direction of motion ofthe mobile, assuming Jakes fading model [1].

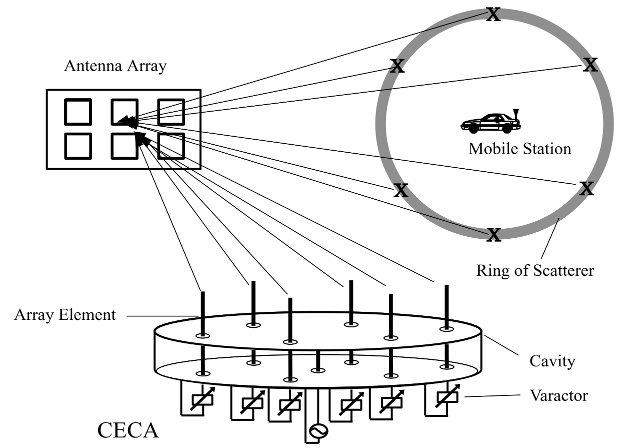

Fig. 10 Scenario of fading simulation.

3.2 Scenario

In this scenario, the base station antenna array is the object of our investigation. In the similar way to Clarke's model, the array elements of CECA comprise time-varying sources with random phases within the region as shown in Fig. 10 [10]. We set the velocity of mobile station to 100 km/h and the carrier frequency to 2.41 GHz so that the maximum Doppler frequency is 223.15 Hz. The time duration between samples is chosen as $(1/f_D)/2^{10} = 4.38\,\mu$s, which is enough for the varactor diode to respond. While the mobile station is moving, the initial phase from scatterers is set by ϕ_m in (16) and phase variation from scatterers can be simulated by controlling the variable capacitor which is loaded to the array elements as (15) and (16). AS relates to an other key factor, the measurement distance between transmitter and receiver. Provided that the receiver is in the Fraunhofer region and base station array's diameter d is 0.5 m, r_a should be more than about 0.432 m to obtain minimum AS, 5°, which can be observed in a macrocell with this criterion [11]. However, this is too big and heavy to handle so that we choose alternative region as the measurement distance and it is in the Fresnel region. An alternative criterion is to focus on the amplitude, and not on the phase so that measurements can be performed successfully in Fresnel region [12], [13]. The criterion is

$$R \geq dD/0.3\lambda \tag{18}$$

Therefore we obtain $R \geq 5.65\lambda$ when base station array's diameter d is 0.5 m.

We assume that base station antenna array separates from transmitter about 6λ.

3.3 Spatial Stochastic Characteristics

As mentioned above, to evaluate antenna arrays, we consider spatial properties, the fading phenomenon and angular spread. The envelope of the signal is Rayleigh distributed while AS depends on the height of the base station antenna

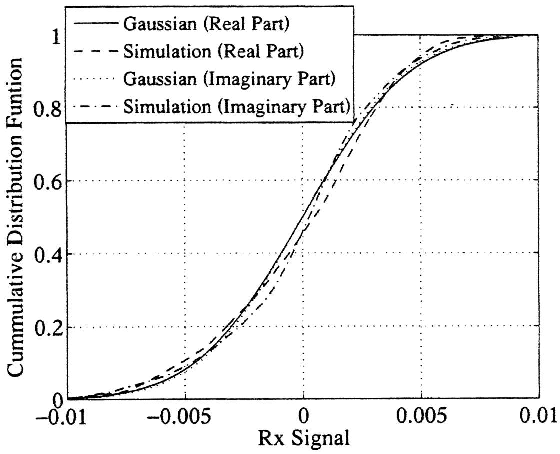

Fig. 11 CDF of real and imaginary part of received signal.

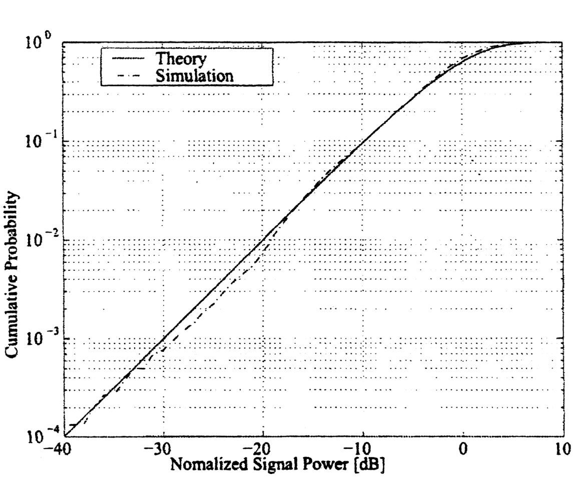

Fig. 12 Cumulative probability of fading signal power.

in the range of 5°–15° [11].

Rayleigh Fading

Figure 11 shows CDF of the received signal and Gaussian. Both CDF of real and imaginary part of the received signal is close to Gaussian. Investigating the power cumulative density function (CDF), as shown in Fig. 12, we see that the envelope of received signal is close to a Rayleigh fading signal. However, the correlation coefficient between real and imaginary part of received signal is about 0.54. That means that though the statistical characteristics are close to Rayleigh fading, the real and imaginary part of the received signal are not independent with each other. Since we know that the received signal does not have an ideal complex-Gaussian distribution, more investigation is necessary to confirm that this simulator can be useful for performance evaluation. Figures 13 and 14 show the received signal level crossing rate (LCR) and average fade duration (AFD). Figures show that though received signal is not a Rayleigh fading signal, it would be valuable to evaluate performance of antenna array. We have come to the conclusion with a well-founded conjecture as shown by the simulation results that this simulator generates the quasi-Rayleigh fading signal which is enough to evaluate an antenna array.

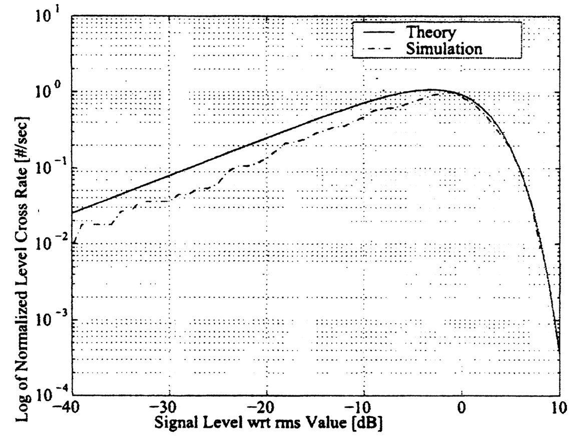

Fig. 13 Level crossing ratio.

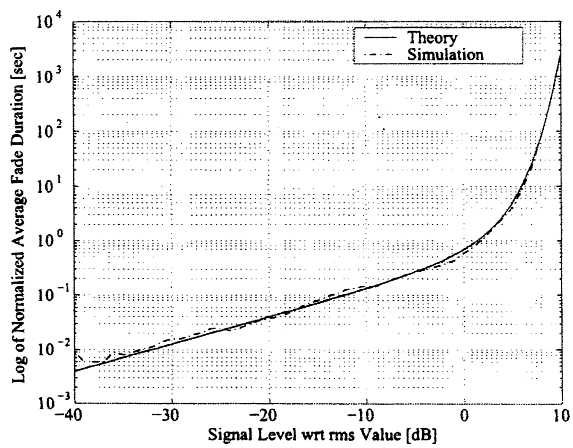

Fig. 14 Average fade duration.

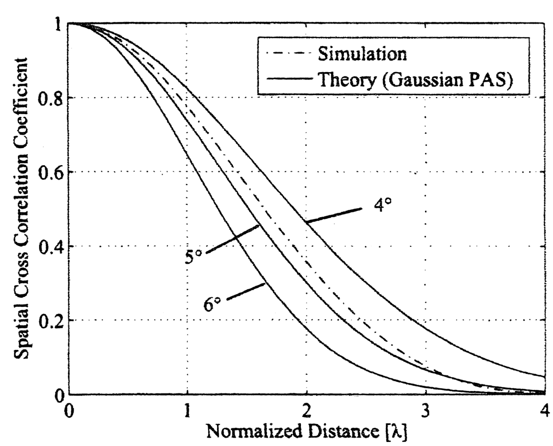

Fig. 15 Spatial cross correlation.

Angular Spreading

The typical method to evaluate AS is to investigate its spatial cross correlation. Figure 15 shows the simulated spatial cross correlation coefficient. Supposing that the power azimuth spectrum has a Gaussian distribution, AS ranges from 4° to 6° defined by its standard deviation [14]. As mentioned above, AS is dependent on the height of the base station antenna and does not have a fixed known quantity. By controlling the radius of the cavity and distance between receiver and transmitter, we obtain several ASs.

4. Conclusion

A cavity-excited circular array (CECA) as a spatial fading simulator has been proposed. Its features, design methodology and measurements on the fabricated CECA have been presented. We showed the computer simulation results on spatial stochastic characteristics to verify CECA as a spatial fading simulator for antenna array. CECA is similar in the stochastic characteristics when using ESPAR since both CDF of the received signal make little difference. However, CECA differs greatly from ESPAR in AS. AS can be controlled by the mode of CECA and the distance between receiver and transmitter so that we can vary ASs. Recently, there are a lot of studies about broadband mobile communication systems. In this paper, we consider only one single frequency so that CECA can not work against broadband systems. The spatial fading simulator for broadband systems is remained as a future work.

Acknowledgment

The author would like to acknowledge Dr. I. Ida for his useful comments and suggestions.

References

[1] W.C. Jakes, Microwave Mobile Communications, John Wiley & Sons, New York, 1974.
[2] U. Martin, "Modeling the mobile radio channel by echo estimation," Frequenz, vol.9-10, no.48, pp.198–212, 1994.
[3] T.S. Rappaport, Wireless Communications, Prentice Hall, New Jersey, 1996.
[4] H. Arai, "Field simulator for Rayleigh/Rician fading reproduction," 2000 IEEE AP-S International Symposium, pp.1552–1555, July 1996.
[5] R. Yamaguchi, "Fading generator using moving scatters," Proc. IEICE Gen. Conf.98', B-1-23, 1998.
[6] T. Ohira, "Electronically steerable passive array radiator (ESPAR) antennas," 2000 IEEE AP-S International Symposium, pp.922–925, July 2000.
[7] K. Sakaguchi, A.L.S. Neves, J. Takada, K. Araki, and T. Ohira, "Spatial fading emulator using an ESPAR antenna structure," Proc. International Symposium on Wireless Personal Multimedia Communications (WPMC'01), vol.2, pp.489–492, Sept. 2001.
[8] EM Software & System, 'FEKO' http://www.feko.co.za, Stelilenbosch, South Africa, 2001.
[9] T. Ohira, "Reactance domain signal processing in parasitic-array antennas (invited)," Asia-Pacific Microwave Conf., APMC2003, WD6-1, 1, pp.290–293, Seoul, Korea, Nov. 2003.
[10] R. Vaughan and J.B. Andersen, Channels, Propagation and Antennas for Mobile Communications, IEE, London, 2003.
[11] K.I. Pedersen, P.E. Mogensen, and B.H. Fleury, "A stochastic model of the temporal and azimuthal dispersion seen at the base station in outdoor propagation environments," IEEE Trans. Veh. Technol., vol.49, no.2, pp.437–447, March 2000.
[12] D.K. Cheng, "On the simulation of Fraunhofer radiation patterns in the Fresnel region," IRE Trans. Antennas Propag., vol.AP-5, no.4, pp.399–402, Oct. 1957.
[13] T.S. Chu, "A note on simulating Fraunhofer radiation patterns in the Fresnel region," IEEE Trans. Antennas Propag., vol.AP-19, no.5, pp.691–692, Sept. 1971.
[14] F. Adachi, M.T. Feeney, A.G. Williamson, and J.D. Parson, "Cross-correlation between the envelopes of 900 MHz signals received at a mobile radio base station site," IEE Proc., vol.133, Pt.F, no.6, pp.506–512, Oct. 1986.

Chulgyun Park was born in Daegu, South Korea in 1971. He received the B.E., M.E degrees in electronic engineering from Hanyang University, South Korea in 1996 and 1998, and D.E. degree in electrical and electronic engineering from Tokyo Institute of Technology, Japan in 2005. His current research interests include development of spatial fading emulator, estimation of smart antenna for mobile station and RF module.

Jun-ichi Takada was born in Tokyo, Japan in 1964. He received the B.E., M.E., and the D.E. degrees from Tokyo Institute of Technology, Japan, in 1987, 1982, respectively. From 1992 to 1994, he has been a Research Associate Professor at Chiba University, Chiba, Japan. From 1994, he has been an Associate Professor at Tokyo Institute of Technology, Tokyo, Japan. His current interests are wireless propagation and channel modelling, array signal processing, ultra-wideband radio, software defined radio, and applied radio instrumentation and measurements. He has been an active member of European COoperation in the field of Scientific and Technical research (COST) action 273 "Towards mobile broadband multimedia networks". He received the Excellent Paper Award and Young Engineer Award from IEICE, Japan, in 1993 and 1994, respectively. He is a member of IEEE, ACES, and ECTI Association Thailand.

Kei Sakaguchi was born in Osaka, Japan, on November 27, 1973. He received the B.E. degree in electrical and computer engineering from Nagoya Institute of Technology, Japan, in 1996, and the M.E. degree in information processing from Tokyo Institute of Technology, Tokyo in 1998. From 2000, he is an Assistant Professor at the Tokyo Institute of Technology. He received the Young Engineer Awards both from IEICE Japan and IEEE AP-S Japan chapter in 2001 and 2002 respectively, and Outstanding Paper Award both from SDR Forum and IEICE in 2004 and 2005 respectively. His current research interests are in MIMO propagation measurement, MIMO communication system, and software defined radio. He is a member of IEEE.

Takashi Ohira received D.E. degree in communication engineering from Osaka University, Osaka, Japan, in 1983. He developed GaAs MMIC transponders and microwave beamforming networks aboard multi-beam communication satellites at NTT Wireless Systems Laboratories, Yokosuka, Japan. Since 1999, he has been engaged in research on wireless adhoc networks and microwave analog smart antennas aboard consumer electronic devices at ATR Adaptive Communications Research Laboratories, Kyoto, Japan. He co-authored Monolithic Microwave Integrated Circuits (Tokyo: IEICE, 1997). He was awarded 1986 IEICE Shinohara Prize and 1998 Japan Microwave Prize. He is a member of URSI Commission C and an IEEE Fellow.